An Innovative Discrete-Time Model Considering Discretization Phase Error and Its Approximation Order Analysis for IM High-Speed Drive

Zhifa Fang, Shinji Doki [1)]

1) Nagoya University, Furo-cho, Chikusa-ku, Nagoya, Aichi, 464-8603, Japan

E-mail: fang.zhifa.r2@nagoya-u.jp, doki@nagoya-u.jp

ABSTRACT: Induction Motors (IMs) are widely used in electric vehicles (EVs) for their simplicity and reliability. The field-oriented control (FOC), which is required to achieve precise torque and swift speed control for EVs, can only be implemented discretely resulting in non-negligible discretization phase errors. This leads to undesirable voltage oscillations that severely deteriorate the current control performance or even disable the current loop as the fundamental-to-control frequency ratio (f_e/f_s) increases. Therefore, an innovative discrete-time IM model accurately modelling voltage oscillations is proposed. The auto current regulator (ACR) designed based on this model significantly enhances IM drive performance in high-speed range. Then, the discretization approximation error of the proposed model is analyzed. Eventually, simulations are conducted to verify the accuracy of the proposed model.

KEY WORDS: high-speed drive, induction motor, discretization phase error, discrete-time model

1. INTRODUCTION

IMs are widely used in EVs due to their cost-efficiency, simple structure, and high reliability. In EVs, motors like traction motors and electric turbochargers require fast torque and speed responses, making FOC essential for achieving the necessary dynamic performance.

Previously, IM drives balanced high-speed operation, computational, and semiconductor performance, but recent demands for higher speeds to achieve miniaturization and high power density have disrupted this balance. High-speed drives require higher control frequencies, constrained by the IGBT/SiC switching frequency, which is limited to several tens of kHz due to semiconductor limitations.

FOC requires the Park transformation to convert current from the $\alpha\beta$ stationary reference frame to the dq synchronous frame for decoupled control of flux and torque. However, real-time flux phase is obtained discretely due to DSP voltage update limitations, causing a time-varying phase error between discretized static $d'q'$-axis and rotational actual dq-axis, which becomes larger as the f_e/f_s increases. This discretization phase error can result in voltage oscillations which significantly degrade control performance and even disable the current loop as f_e/f_s increases.

To address this, some simple phase compensation methods, such as a half-step compensation [(1)], were proposed. However, these methods assume voltage commands match the average actual voltage over a control period, and thus could not address the discretization error fundamentally. As a result, a precise solution would accurately model the discretization phase error in the IM's discrete-time model [(2)(3)].

In this paper, causes of the discretization phase error are first explained in detail in Section 2. Then, the traditional discrete-time IM model and the half-step compensation method are introduced in Section 3. In Section 4, an innovative discrete-time IM model will be proposed by accurately modelling the voltage oscillation caused by discretization phase error. Subsequently, approximation error analysis and simulations are conducted in Section 5 and Section 6, followed by conclusion in Section 7.

2. DISCRETIZATION PHASE ERROR

2.1 Discrete Park Transformation

The block diagram of the FOC-based discrete-time IM drive system is exhibited in Fig.1. To achieve individual control of torque and flux, the stator currents in the uvw three-phase symmetrical reference frame must be transformed into dq synchronous reference frame by the Clarke transformation and the Park transformation. The Clarke transformation is a constant transformation thereby causing no problems after discretization. In contrast, the Park transformation necessitates the phase $\theta(t)$ of the actual dq -axis, which is continuously rotating. However, the phase for Park transformation can only be attained discretely, denoted as $\theta[k]$ in discrete $d'q'$-axis, leading to the discretization phase error between the actual dq-axis and the discrete $d'q'$-axis.

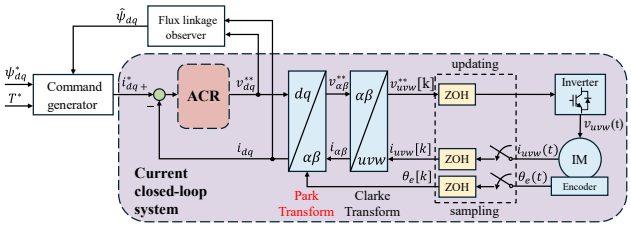

Fig.1 Block diagram of the discrete-time FOC control.

2.2 Causes of the discretization phase error

Fig.2 shows the entire discrete-time control process of an IM with the control period T_s. The discretization phase error can be considered to consist of two parts lasting two control periods. First, the current and the electric angle are sampled at kT_s, denoted as $i_{dq}[kT_s]$, $\theta[kT_s]$, and then are utilized to compute the output voltage command $v_{dq}^*[(k+1)T_s]$ on the discrete $d'q'$-axis before the next sampling point. However, the actual dq axis continuously rotates resulting in a $\omega_e T_s$ phase delay in a control period which is known as the inverter delay. Then, the voltage command $v_{dq}^*[(k+1)T_s]$ is applied to the stator winding at $(k+1)T_s$ and must be sustained constant during the subsequent control period as the ZOH effect. This ZOH effect can cause the continuous phase delay between the $d'q'$-axis and dq axis, as depicted in Fig.3 (a), resulting in the output voltage oscillating in the perspective of the actual dq axis as shown in Fig.3 (b).

Even though the $\omega_e T_s$ phase error caused by inverter delay can by adding a $e_e^{-j\omega_e T_s}$ item before the voltage command, the phase error caused by the ZOH effect has not been solved fundamentally.

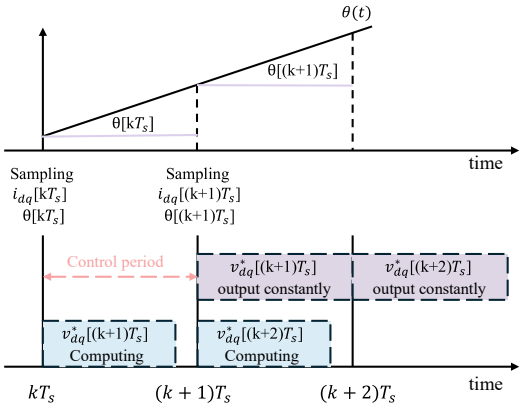

Fig.2 Block diagram of discrete-time control process.

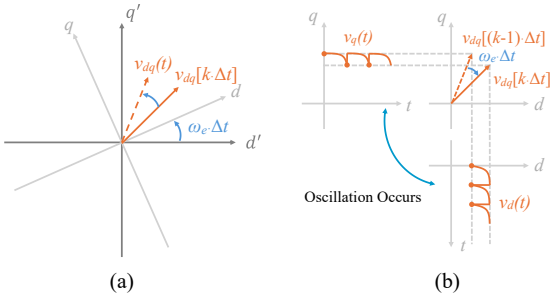

Fig.3 Voltage oscillation caused by the ZOH effect.

3. TRADITIONAL DISCRETE-TIME IM MODEL AND ACR WITH STEP COMPENSATION

3.1 Traditional discrete-time IM model on continuous dq-axis

The IM model in continuous time dq synchronous reference frame is expressed as:

$$\frac{d}{dt}\begin{bmatrix}\boldsymbol{i}_{sdq}\\ \boldsymbol{\psi}_{rdq}\end{bmatrix} = \boldsymbol{A}\begin{bmatrix}\boldsymbol{i}_{sdq}\\ \boldsymbol{\psi}_{rdq}\end{bmatrix} + \boldsymbol{B}\,\boldsymbol{v}_{dq} \tag{1}$$

$$\boldsymbol{A} = \begin{bmatrix}a_{11i}\mathbb{I} + a_{11j}\mathbb{J} & a_{12i}\mathbb{I} + a_{12j}\mathbb{J}\\ a_{21i}\mathbb{I} & a_{22i}\mathbb{I} + a_{22j}\mathbb{J}\end{bmatrix};\ \boldsymbol{B} = \begin{bmatrix}\frac{1}{\sigma L_s}\mathbb{I}\\ \mathbb{O}\end{bmatrix}, \tag{2}$$

where

$$a_{11i} = -\frac{R_s}{\sigma L_s} - \frac{(1-\sigma)R_r}{\sigma L_r};\ a_{11j} = -\omega_e;\ a_{12i} = \frac{MR_r}{\sigma L_r^2 L_s}; \tag{3}$$

$$a_{12j} = -\frac{M\omega_{re}}{\sigma L_r L_s};\ a_{21i} = \frac{MR_r}{L_r};\ a_{22i} = -\frac{R_r}{L_r};\ a_{22j} = -\omega_s; \tag{4}$$

$$\mathbb{O} = \begin{bmatrix}0 & 0\\ 0 & 0\end{bmatrix};\ \mathbb{I} = \begin{bmatrix}1 & 0\\ 0 & 1\end{bmatrix};\ \mathbb{J} = \begin{bmatrix}0 & -1\\ 1 & 0\end{bmatrix}. \tag{5}$$

The $\boldsymbol{i}_{sdq} = [i_{sd}\quad i_{sq}]^T$ and $\boldsymbol{\psi}_{rdq} = [\psi_{rd}\quad \psi_{rq}]^T$ are the stator current and rotor flux, of which the lower script 's' and 'r' represent the stator and rotor side, respectively.

The $\omega_s = \omega_e - \omega_{re}$ is the slip frequency, where ω_{re}, ω_e are rotor electrical angular velocity and electrical angular velocity; R_s, R_r are the resistance of the stator and rotor; L_s, L_r are the inductance of the stator and rotor; M is the mutual inductance; $\sigma = 1 - \frac{M^2}{L_s L_r}$ is the total leakage coefficient.

The discrete-time IM model can be obtained by discretizing equation (1) using the ZOH and Pade approximant.

$$\boldsymbol{A_d} = e^{\boldsymbol{A}T_s} = \boldsymbol{I} + \boldsymbol{A}T_s + \frac{1}{2!}\boldsymbol{A}^2T_s^2 + \cdots \tag{6}$$

$$\boldsymbol{B_d} = \int_0^{T_s} e^{\boldsymbol{A}\tau'}d\tau'\boldsymbol{B} = \boldsymbol{I}\boldsymbol{B}T_s + \frac{1}{2!}\boldsymbol{A}\boldsymbol{B}T_s^2 + \frac{1}{3!}\boldsymbol{A}^2\boldsymbol{B}T_s^3 + \cdots \tag{7}$$

The $\boldsymbol{A_d}$ and $\boldsymbol{B_d}$ should be considered to approximate to higher orders to adapt the high-speed drive application. Without loss of generality, considering the $\boldsymbol{A}$ and $\boldsymbol{B}$ are approximated to high orders and let $\psi_{rq} = 0$, $\boldsymbol{A_d}$ and $\boldsymbol{B_d}$ have following forms.

$$\boldsymbol{A_d} = \begin{bmatrix}a_{11} & a_{12} & a_{13}\\ -a_{12} & a_{11} & a_{14}\\ a_{31} & a_{32} & a_{33}\end{bmatrix},\ \boldsymbol{B_d} = \begin{bmatrix}b_{11} & b_{12}\\ -b_{12} & b_{11}\\ b_{31} & b_{32}\end{bmatrix} \tag{8}$$

3.2 ACR design based on traditional model

The state feedback decoupling method is adopted to eliminate the cross-coupling responses between the d-axis and q-axis, which is expressed as:

$$\begin{bmatrix}v_d^{**}\\ v_q^{**}\end{bmatrix} = \boldsymbol{B_0}^{-1}\begin{bmatrix}v_d^{*}\\ v_q^{*}\end{bmatrix}, \tag{9}$$

where v_d^{**}, v_q^{**} are voltage commands output to stator windings; $\boldsymbol{B_0^{-1}}$ accounts for the decoupling of voltage commands in different axis, where $\boldsymbol{B_0}$ is parts of $\boldsymbol{B_d}$ and expressed as:

$$\boldsymbol{B_0} = \begin{bmatrix} b_{11} & b_{12} \\ -b_{12} & b_{11} \end{bmatrix} \tag{10}$$

and its corresponding inverse matrix is

$$\boldsymbol{B_0^{-1}} = \frac{1}{b_{11}^2 + b_{12}^2} \begin{bmatrix} b_{11} & -b_{12} \\ b_{12} & b_{11} \end{bmatrix}. \tag{11}$$

v_d^*, v_q^* are voltage commands after performing the decoupling of the $\boldsymbol{A_d}$ by following expressions:

$$\begin{cases} v_d^* = \tilde{v}_d - a_{12} i_q \\ v_q^* = \tilde{v}_q + a_{12} i_d - a_{14} \psi_d \end{cases}, \tag{12}$$

where $\tilde{v}_d$, $\tilde{v}_q$ are the voltage commands calculated through the PI regulator. The PI controller discretized by the Forward Euler method is

$$G_c(z) = k_p + \frac{k_i T_s}{z - 1}, \tag{13}$$

where k_p, k_i are the PI gains and usually are tunned by performing the pole-zero cancellation.

$$\begin{cases} k_p = \omega_{cc} T_s \\ k_i = \omega_{cc}(1 - a_{11}) \end{cases} \tag{14}$$

3.3 Traditional step compensation for the discretization phase error

Traditional phase step compensation is derived from modeling and compensating for the discretization phase error between the discrete $d'q'$-axis and the actual dq-axis according to the simple criterion: the average voltage in a stator must equal the voltage command after compensation. The practical approach is rotating voltage commands phase $\frac{1}{2}\omega_e T_s$.

4. PROPOSED DISCRETE-TIME IM MODEL AND ACR

4.1 Proposed discrete-time IM model on discrete dq-axis

During a control period, while constant voltage commands are applied, the actual dq-axis continues to rotate, causing voltage oscillations from its perspective. Therefore, it is necessary to left multiply an opposite rotation matrix to the voltage command matrix to transform the actual dq-axis to the discrete $d'q'$-axis during the integration term of $\boldsymbol{B}$ discretization, making all variables in discrete-time model are on the same discrete $d'q'$-axis.

$$\boldsymbol{B_d'} = \int_0^{T_s} e^{\boldsymbol{A}\tau'} \boldsymbol{R}^T(\omega_e(T_s - \tau'))d\tau' \boldsymbol{B} \tag{15}$$

where the rotation matrix $\boldsymbol{R}(\theta)$ is

$$\boldsymbol{R}(\theta) = \begin{bmatrix} \cos(\theta) & -\sin(\theta) \\ \sin(\theta) & \cos(\theta) \end{bmatrix}. \tag{16}$$

According to the Pade approximant, $\boldsymbol{B_d'}$ can be approximated as

$$\boldsymbol{B_d'} = \boldsymbol{BV_0} + \boldsymbol{ABV_1} + \frac{1}{2!}\boldsymbol{A^2BV_2} + \frac{1}{3!}\boldsymbol{A^3BV_3} + \cdots \tag{17}$$

$$\boldsymbol{V_n} = \int_0^{T_s} \tau'^n \boldsymbol{R}^T(\omega_e(T_s - \tau'))d\tau' \tag{18}$$

where $n = 0, 1, \cdots$ respresents the approximation order. The voltage oscillation due to the ZOH effect is modeled by $\boldsymbol{V_n}$.

In conclusion, only the discretization process of $\boldsymbol{B}$ is improved, which can be expressed as:

$$\boldsymbol{B_d'} = \begin{bmatrix} b_{11}' & b_{12}' \\ -b_{12}' & b_{11}' \\ b_{31}' & b_{32}' \end{bmatrix}. \tag{19}$$

4.2 ACR design based on proposed model

The ACR design process for proposed model is the same as that for traditional model following the Section 3.2. The voltage commands applied to the stator is

$$\begin{bmatrix} v_d^{**} \\ v_q^{**} \end{bmatrix} = \boldsymbol{B_0'^{-1}} \begin{bmatrix} v_d^* \\ v_q^* \end{bmatrix},$$

where $\boldsymbol{B_0'}$ is parts of $\boldsymbol{B_d'}$ and the $\boldsymbol{B_0^{-1}}$ expressed as:

$$\boldsymbol{B_0^{-1}} = \frac{1}{b_{11}'^2 + b_{12}'^2} \begin{bmatrix} b_{11}' & -b_{12}' \\ b_{12}' & b_{11}' \end{bmatrix}.$$

The $\boldsymbol{B_0^{-1}}$ accounts for the decoupling of the voltage cross-coupling caused by the ZOH effect. In addition, the decoupling of the $\boldsymbol{A_d}$ and the gain tuning of the PI controller is the same as the ACR designed based on the traditional model from (12) to (14), since the discretization process is unchanged in proposed model.

5. ANALYSIS OF APPROXIMATION ORDER

The IM parameters are provided in Table 1, which is subsequently used for simulation in the next section.

Table 1 Parameters of the IM and ACR.

Parameter	Value	Parameter	value
R_s	0.69 [Ω]	M	0.114 [H]
R_r	1.96 [Ω]	Poles	4
L_s	0.118 [H]	ω_{cc}	2000 [rad/s]
L_r	0.118[H]	f_s	10,000 [Hz]

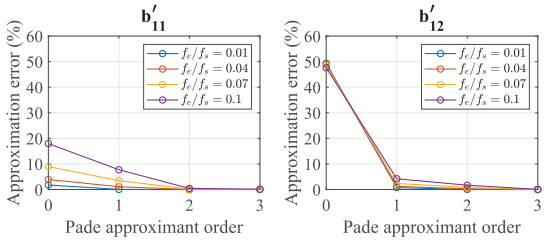

Fig.4 Approximation error of $\boldsymbol{B}_d$ in different f_s/f_e ratio.

The relationship between the Pade approximation order and the approximation error of the $\boldsymbol{B_d'}$ elements with the increase of f_e/f_s is illustrated in Fig.4. The b_{12}' represents the voltage cross-coupling, of which approximation errors are relatively insensitive to f_e/f_s. Thus, for IM high-speed drives, it is recommended to prioritize approximating b_{12}' to the first order, and then gradually

increase the approximation order based on the desired performance of the current closed-loop system. Besides, the b'_{11} is suggestable approximated over the second order to promise an acceptable approximation error in high-speed range.

6. SIMULATION

The IM parameter for simulation is exhibited in Table 1. To minimize the effect of discretization error in the $\boldsymbol{A}$ matrix, the $\boldsymbol{A}$ matrix is approximated to the third order. In addition, $\boldsymbol{B_d}$ and $\boldsymbol{B'_d}$ are simultaneously approximated in the same order for comparison. The d-axis current was set constant at 50A, and a step command from 100A to 300A was applied to the q-axis current at 1 second. Additionally, current step experiments were conducted at 3000RPM, 12000RPM, 20000RPM, and 30000RPM, where the f_e/f_s approximates 0.01, 0.04, 0.07, and 0.1 individually, to observe the changes of decoupling performance and overshoot according to the increase of f_e/f_s.

The simulation results, where $\boldsymbol{B'_d}$ is approximated to the second and third order, are illustrated in Fig.5 and Fig.6, respectively. When the ACR is designed based on the traditional discrete-time IM model, overshoots caused by voltage cross-coupling considerably increase as f_e/f_s increases. In contrast, the proposed discrete-time IM model effectively suppresses the overshoots, which remain stable even as the f_e/f_s increases. This demonstrates that the voltage cross-coupling results from the discretization phase error is accurately modeled.

From Fig.7, it also shows excellent control performance when the diagonal items and cross-coupling items of $\boldsymbol{B_d}$ are approximated to the second and first order, individually. The results suggest reducing computational efficiency by approximating the cross-coupling items to the first order while ensuring the decoupling performance, of which approximate 20% floating-point operations can be reduced.

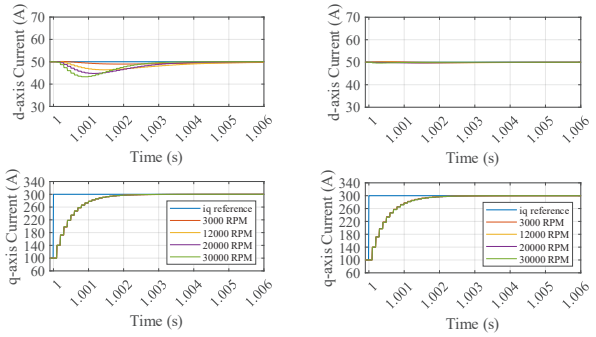

(a) Traditional IM model with a half-step compensation. (b) Proposed IM model.

Fig.5 Current step responses when $\boldsymbol{B_d}$ is approximated at the second order.

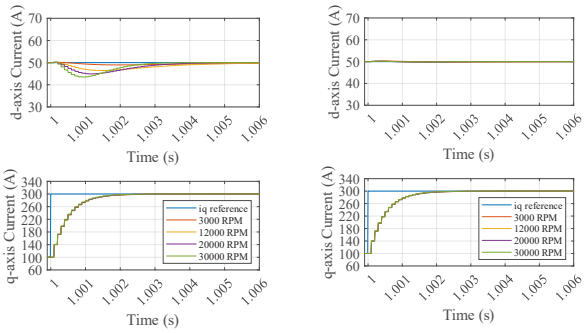

(a) Traditional IM model with a half-step compensation. (b) Proposed IM model

Fig.6 Current step responses when $\boldsymbol{B_d}$ is approximated at the third order.

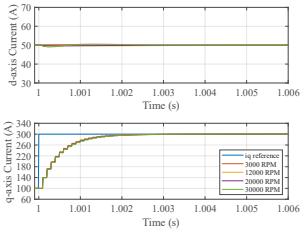

Fig.7 Current step responses when the diagonal items and cross-coupling items are approximated in the second and first order.

7. CONCLUSIONS

This paper proposed an innovative discrete-time IM model that accurately models the voltage oscillation caused by discretization phase errors. Then, approximation error analysis suggests reducing computational efficiency by approximating the cross-coupling elements to a relatively lower order. Eventually, the effectiveness of the proposed model and the recommended computation-efficient method were verified by simulations.

ACKNOWLEDGMENT

The author Zhifa Fang is receiving the scholarship from the China Scholarship Council under Grant No. 202306880002.

REFERENCES

(1) L. Wu et al., “Design of Complex Vector Controller for High-Power Induction Machine Drive,” IEEE Trans. Transp. Electrific., vol. 10, no. 1, pp. 1816–1826, Mar. 2024.

(2) M.Inoue, S.Doki ”Discrete-time PMSM Modeling Including Park Transformation and Decoupling Control Based on the Proposed Model”, IEEJ Transactions on Industry Applications, Vol.139 No.7 pp.637-644, 2019 (in Japanese)

(3) T. Takeuchi and S. Doki, "Current Vector Control System Based on a New Discrete dq-Axis IM Model for High Speed Drive," 2022 International Power Electronics Conference (IPEC-Himeji 2022- ECCE Asia), Himeji, Japan, 2022, pp. 783-788.